Biochemical Pharmacology 81 (2011) 856–865

Contents lists available at ScienceDirect

Biochemical Pharmacology

journal homepage: www.elsevier.com/locate/biochempharm

7-Chloro-6-piperidin-1-yl-quinoline-5,8-dione (PT-262), a novel ROCK inhibitor blocks cytoskeleton function and cell migration

Chih-Chien Tsai [a,b], Huei-Fang Liu [a], Kai-Cheng Hsu [a,c], Jinn-Moon Yang [a,c], Chinpiao Chen [d], Kuang-Kai Liu [a], Tzu-Sheng Hsu [b], Jui-I. Chao [a,e,*]

[a] Department of Biological Science and Technology, National Chiao Tung University, Hsinchu 30068, Taiwan
[b] Institute of Pharmacology and Toxicology, Tzu Chi University, Hualien 970, Taiwan
[c] Institute of Bioinformatics and Systems Biology, National Chiao Tung University, Hsinchu 30068, Taiwan
[d] Department of Chemistry, National Dong Hwa University, Hualien 970, Taiwan
[e] Institute of Molecular Medicine and Bioengineering, National Chiao Tung University, Hsinchu 30068, Taiwan

ARTICLE INFO

Article history:
Received 30 November 2010
Accepted 13 January 2011
Available online 26 January 2011

Keywords:
PT-262
ROCK
Cell migration
Cytoskeleton
Lung cancer

ABSTRACT

The 5,8-quinolinediones are precursors for producing multiple types of bioactive products. In this study, we investigated a new compound derived from 5,8-quinolinediones, 7-chloro-6-piperidin-1-yl-quinoline-5,8-dione (designated as PT-262), which markedly induced cytoskeleton remodeling and migration inhibition in lung carcinoma cells. Comparison with various cytoskeleton inhibitors, including paclitaxel, colchicine and phallacidin, the cell morphology following treatment with PT-262 was similar to phallacidin on the cell elongation and abnormal actin polymerization. However, PT-262 did not directly bind to actin filaments. ROCK (Rho-associated coiled-coil forming protein kinase) is a downstream effector of RhoA to mediate the phosphorylation of myosin light chain (MLC) and cytoskeleton reorganization. The RhoA–ROCK–MLC pathway has been shown to promote cancer cell migration and metastasis. Interestingly, PT-262 was more effective on inhibiting ROCK kinase activities than specific ROCK inhibitors Y-27632 and H-1152. PT-262 induced cytoskeleton remodeling and migration inhibition in A549 lung carcinoma cells. The total MLC and phosphorylated MLC proteins and stress fibers were blocked after treatment with PT-262. Nonetheless, the RhoA protein and GTPase activity were not altered by PT-262. A computational model suggests that PT-262 interacts with the ATP-binding site of ROCK protein. Together, these findings demonstrate that PT-262 is a new ROCK inhibitor.

1. Introduction

The reorganization of cytoskeleton plays important roles in the regulation of cancer cell migration and metastasis. The RhoGTPases are key regulators of cytoskeleton dynamics [1,2]. The RhoGTPase family members include RhoA, Rac1, and Cdc42 in mammalian cells. RhoA is involved in the regulation of cytoskeleton reorganization and focal adhesion, whereas Rac1 and Cdc42 work together at the regulation of cell leading edges to form lamellipodia and filopodia [3,4]. RhoA is a key family of RhoGTPases that participates in cancer migration and metastasis [5,6]. Overexpression of RhoA has been found in a variety of cancers including, lung, bladder, testicular, ovarian, colon, and breast [7]. ROCK (Rho-associated coiled-coil forming protein kinase) is a RhoA downstream protein [5]. There are two isoforms of ROCK, known as ROCK1 and ROCK2 [8]. Both ROCK1 and ROCK2 can regulate the activity of myosin light chain (MLC) proteins by direct MLC phosphorylation [9,10]. Cell migration of actomyosin contractility is mediated by the phosphorylation of MLC for cell movement [1]. Moreover, ROCK has been shown to induce the stress fiber formation and cancer cell migration and metastasis [5,11,12]. Thus, the development of strategies or drugs to block the RhoA–ROCK pathway is highly desirable for cancer therapy.

Y-27632, [(+)-(R)-trans-4-(1-aminoethyl)-N-(4-pyridyl)cyclohexane carboxamide dihydrochloride], is a specific ROCK inhibitor [10,13]. The inhibiting ROCK mechanism of Y-27632 is through binding to the catalytic site of ROCK by competing with the ATP binding site [14]. Inhibition of ROCK by Y-27632 blocks cancer cell

Abbreviations: ROCK, Rho-associated coiled-coil forming protein kinase; MLC, myosin light chain; MBS, myosin binding subunit; DMSO, dimethyl sulfoxide; PI, propidium iodide; MTT, 3-(4,5-dimethyl-thiazol-2-yl) 2,5-diphenyl tetrazolium bromide; FBS, fetal bovine serum; ERK, extracellular signal-regulated kinase; PBS, phosphate-buffered saline; F-actin, actin filament.

* Corresponding author at: Department of Biological Science and Technology, National Chiao Tung University, 75, Bo-Ai Street, Hsinchu 30068, Taiwan.
Tel.: +886 3 5712121x56965; fax: +886 3 5131309.
E-mail address: jichao@faculty.nctu.edu.tw (J.-I. Chao).

0006-2952/$ – see front matter © 2011 Elsevier Inc. All rights reserved.
doi:10.1016/j.bcp.2011.01.009

migration, invasion and metastasis [15–17]. Y-27632 inhibits ROCK kinase activity to disrupt networks and remodeling of actin filaments in cancer cells [15,17]. Furthermore, Y-27632 reduces cancer invasion by reducing the levels of matrix metalloproteinases (MMPs) such as MMP-2 and MMP-9 [17]. In addition, H-1152, (S)-(+)-2-methyl-1-[(4-methyl-5-isoquinoline)sulfonyl]-homopiperazine, is another specific ROCK inhibitor derived from isoquinoline–sulfonamide analogues similar to Y-27632 by binding to catalytic site of ROCK [10,18].

The 5,8-quinolinediones are useful precursors for producing multiple types of bioactive products [19]. The derivatives of quinolinediones have been shown to possess many biological activities including anti-tumor and anti-microbial actions. 6-Anilino-5,8-quinolinedione (LY83583) is an inhibitor of guanylyl cyclase that can reduce cancer cell proliferation [20]. 6-Chloro-7-(2-morpholin-4-ylethylamino)quinoline-5,8-dione (NSC 663284), an inhibitor of CDC25 protein phosphatases, induced cell cycle arrest by reducing CDC2 activation in cancer cells [21]. Lavendamycin is a bacterially derived quinolinedione that displays significant anticancer activities [22]. 7-Chloro-6-piperidin-1-yl-quinoline-5,8-dione (designated as PT-262) is a new derivative of 5,8-quinolinedione, which induced apoptosis associated with inhibiting CDC2 and ERK phosphorylation [23].

In this study, we investigated a new ROCK inhibitor, PT-262, which inhibited cytoskeleton function, stress fiber formation, and migration in human lung carcinoma cells. In addition, PT-262 was more effective in inhibiting ROCK kinase activity and cancer cell migration than Y-27632 and H-1152. PT-262 can be developed as a novel ROCK inhibitor.

2. Materials and methods

2.1. Materials

The chemical synthesis of PT-262 was according to a previous study [23]. PT-262 was dissolved in 100% dimethyl sulfoxide (DMSO). The concentration of DMSO was <0.2% in the control and drug-containing media in each experiment. Hoechst 33258, propidium iodide (PI), 3-(4,5-dimethyl-thiazol-2-yl)2,5-diphenyl tetrazolium bromide (MTT), colchicine, paclitaxel, and the Cy3-labeled mouse anti-β-tubulin, gelatin, fibronectin and Y-27632 were purchased from Sigma Chemical Co. (St. Louis, MO). Anti-ERK-2 (C-14) and anti-RhoA (sc-179) were purchased from Santa Cruz Biotechnology, Inc. (Santa Cruz, CA). BODIPY FL phallacidin (B-607) and Lipofectamine™ 2000 were purchased from Invitrogen (Carlsbad, CA). The Cy5-labeled goat anti-rabbit IgG was purchased from Amersham Pharmacia Biotech (Little Chalfont Buckinghamshire, UK). Anti-phospho-MLC (serine-19), anti-MLC, and anti-ROCK1 antibodies were purchased from Cell Signaling Technology, Inc. (Beverly, MA). H-1152 was purchased from Merck Calbiochem (San Diego, CA).

2.2. Cell culture

The A549 cell line (ATCC, #CCL-185) was derived from a non-small cell lung adenocarcinoma tumor. A549 cells were cultured in RPMI-1640 medium (Invitrogen) supplemented with 10% fetal bovine serum (FBS), 100 units/ml penicillin, 100 μg/ml streptomycin, and L-glutamine (0.03%, w/v). The cells were maintained at 37 °C and 5% CO_2 in a humidified incubator (310/Thermo, Forma Scientific, Inc., Marietta, OH).

2.3. Cytoskeleton staining and confocal microscopy

The cells were cultured on coverslips, which were kept in a 60-mm Petri dish for 16–20 h. At the end of treatment, the cells were washed with isotonic PBS (pH 7.4), and then the cells were fixed in 4% paraformaldehyde solution in PBS for 1 h at 37 °C. Subsequently, the coverslips were washed three times with PBS, and non-specific binding sites were blocked in PBS containing 10% FBS and 0.3% Triton X-100 for 1 h. Actin filament (F-actin) and β-tubulin were stained with 20 U/ml BODIPY FL phallacidin and anti-β-tubulin Cy3 (1:50) for 30 min at 37 °C, respectively. Finally, the nuclei were stained with 2.5 μg/ml Hoechst 33258 for 30 min. The samples were examined under a Leica confocal laser scanning microscope (Mannheim, Germany) that equipped with an UV laser (351/364 nm), an Ar laser (457/488/514 nm), and a HeNe laser (543 nm/633 nm). The fluorescence images were displayed through the frame store in the computer, and the cell length was calculated using a Leica confocal software (Ver. Lite).

2.4. Bio-atomic force microscopy (Bio-AFM)

To observe the cytoskeleton alteration and cell elongation by PT-262, the cells were analyzed by a BD CARV II confocal microscope combined a NanoWizard Bio-AFM (JPK Instruments, Berlin). Bio-AFM was mounted on an inverted microscope, TE-2000-U (Nikon, Japan). The silicon nitride non-sharpened cantilever was used by a nominal force constant of 0.06 N/m (DNP-20, Veeco). The images were scanner by using contact mode. Line scan rates are varied from 0.5 to 2 Hz.

2.5. Actin polymerization assay

Actin polymerization assays *in vitro* (BK003) were purchased from Cytoskeleton, Inc. (Denver, CO). After treatment with or without PT-262, the actin polymerization reaction was analyzed according to the manufacturer's recommendations. Phallacidin was used as a positive control in actin polymerization. Briefly, the actin polymerization assays were based on the enhanced fluorescence of pyrene-conjugated actin that occurs during polymerization. The enhanced fluorescence were measured by pyrene monomer globular-actin (G-actin) formed polymer pyrene F-actin in a fluorometer at excitation wavelength 365 nm and emission wavelength 407 nm.

2.6. Boyden chamber analysis

The cell migration was examined by the Boyden chamber analysis. Boyden's chamber system was used two chambers separated by a collagen coated 8 μm pore size polycarbonate membrane. Briefly, the polycarbonate filter of 8 μm pore size was soaked in 0.5 M acetic acid overnight. The filter was washed with distilled water and then incubated for 16 h in a 100 μg/ml gelatin solution and air dried. The gelatin coating filters were incubated again in a 10 μg/ml fibronectin solution for 2 h. The tested drugs were added to the bottom well of a Bodyen chamber. Cells on the upper surface of the filters were carefully removed with a cotton swab. Cells on the lower surface were counted after stained with hematoxylin under a light microscope.

2.7. Wound healing assay

The cells were cultured in six-well plate for 24 h overnight, resulting in a monolayer that was more than 90% confluent. The cell monolayer was scraped with a 200 μl pipette tip to generate the wound of 6–7 mm. Thereafter, the cells were treated with or without PT-262, washed with PBS, and then re-cultured in fresh medium for various periods. Photographs were taken at 8 and 24 h on the same position of the wound.

2.8. ROCK kinase assay

A549 cells were treated with or without PT-262, Y-27632 or H-1152. After drug treatment, the cell lysates were diluted in kinase buffer and allowed to phosphorylate the bound substrate myosin binding subunit (MBS). The amount of MBS was calculated in a binding reaction with a horseradish peroxidase conjugate of AF20, an anti-phospho-MBS threonine-696 specific antibody, which catalyzes the conversion of the chromogenic substrate tetramethylbenzidine from a clear to a blue-colored solution. The color reaction product was quantified by measuring the absorbance at 450 nm using a VERSAmax microtiter plate reader (Molecular Devices Corp., Sunnyvale, CA).

2.9. Western blot analysis

Western analyses of RhoA, ERK-2, MLC, phospho-MLC, and ROCK1 were performed using specific antibodies. At the end of the treatment, the cells were lysed in ice-cold whole cell extract buffer containing protease inhibitors as described [24]. Briefly, equal amounts of proteins in samples were subjected to electrophoresis using 10–12% sodium dodecyl sulfate-polyacrylamide gels. After

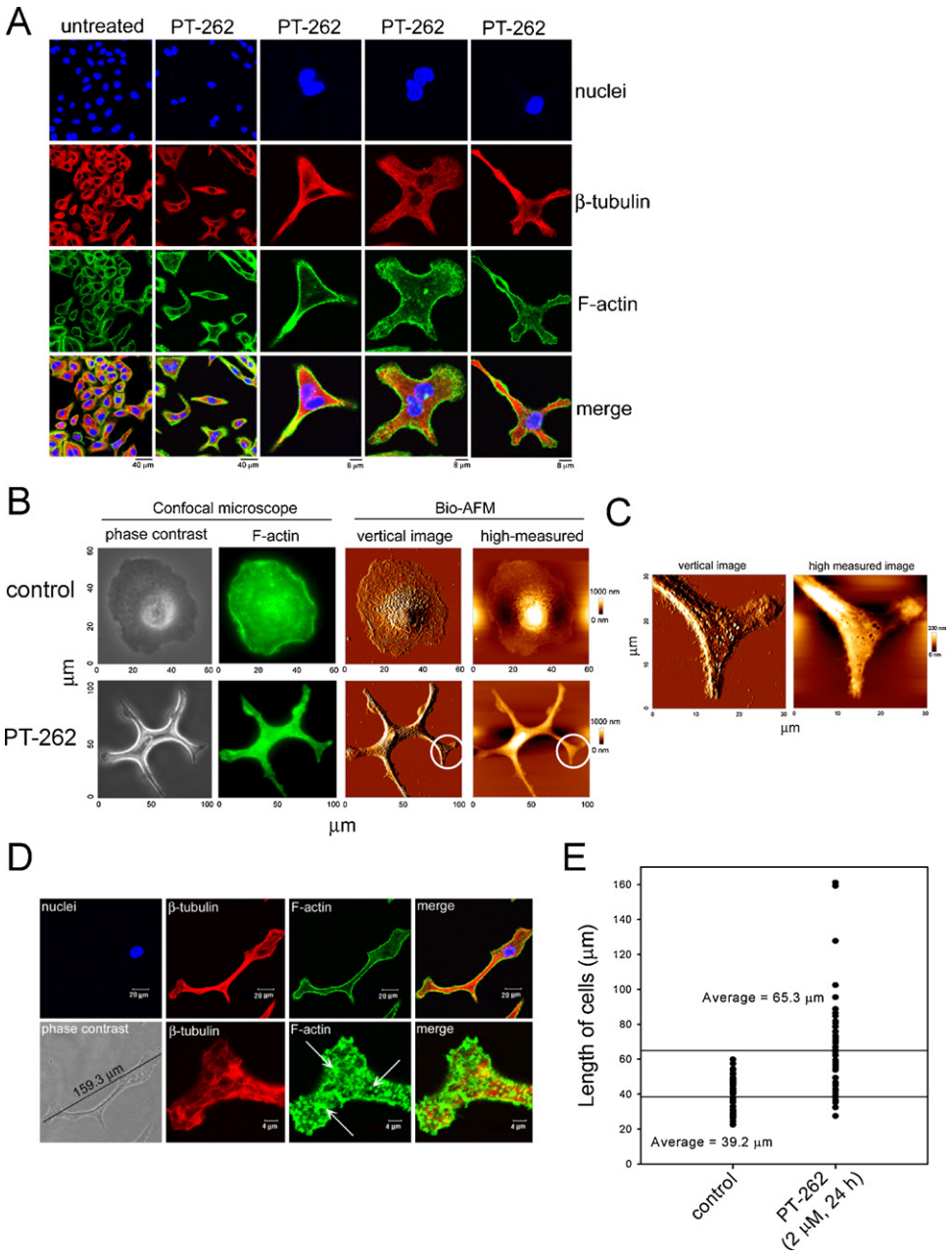

Fig. 1. Effect of PT-262 on the cytoskeleton remodeling and cell elongation in lung carcinoma cells. (A) A549 cells were treated with or without 2 μM PT-262 for 24 h. At the end of treatment, β-tubulin, F-actin, and nuclei were stained with Cy3-labeled mouse anti-β-tubulin, BODIPY FL phallacidin, Hoechst 33258, respectively. The β-tubulin displayed a red color. The blue color indicated the location of nuclei or chromosomes. The green color indicated the location of F-actin. (B) The untreated or PT-262-treated cells were analyzed by confocal microscope-combined Bio-AFM. The green color indicated the location of F-actin proteins. (C) The amplified pictures were obtained from circle marks of (B). (D) A549 cells were treated with or without 2 μM PT-262 for 24 h. The β-tubulin, F-actin, and nuclei were stained with the Cy3-labeled mouse anti-β-tubulin, BODIPY FL phallacidin, Hoechst 33258, respectively. The treated or untreated cells were subject to confocal microscopy analysis. The arrows indicate the F-actin spikes. (E) The cell length was measured using Leica confocal software. The average cell length (long diameter) was calculated from three separate experiments. (For interpretation of the references to color in this sentence, the reader is referred to the web version of the article.)

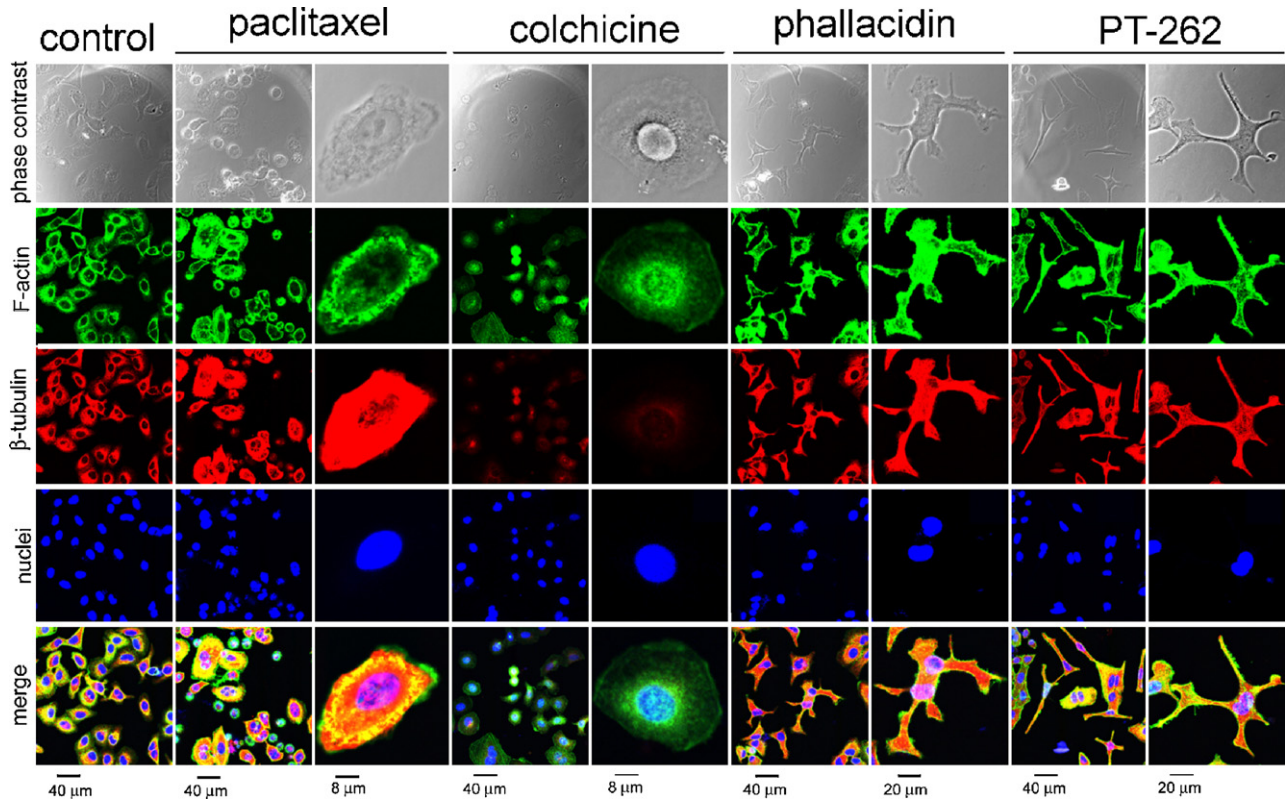

Fig. 2. Comparison of various cytoskeleton blockers on the cytoskeleton alteration and cell morphology in lung carcinoma cells. A549 cells were treated with or without cytoskeleton blockers. β-tubulin, F-actin, and nuclei were stained with Cy3-labeled mouse anti-β-tubulin, BODIPY FL phallacidin, Hoechst 33258, respectively. The treated or untreated cells were subject to confocal microscopy analysis. The β-tubulin displayed a red color. The blue color indicated the location of nuclei or chromosomes. The green color indicated the location of F-actin. (For interpretation of the references to color in this sentence, the reader is referred to the web version of the article.)

electrophoretic transfer of proteins onto polyvinylidene difluoride membranes, they were sequentially hybridized with primary antibody and followed with a horseradish peroxidase-conjugated second antibody (Santa Cruz Biotechnology, Inc., Santa Cruz, CA). Finally, the protein bands were visualized using the enhanced chemiluminescence detection system (NEN, Boston, MA).

2.10. RhoA GTPase activity assay

Activated GTP-RhoA proteins were detected by a pull-down assay kit (Upstate Biotechnology, Lake Placid, NY) for Rho–GTP bound to the Rho-binding domain (RBD) of Rhotekin, a downstream effector of Rho. Rho activation kit used the Rhotekin-RBD fused with GST to affinity precipitate cellular Rho–GTP. Briefly, the cells were treated with or without PT-262. At the end of treatments, the cell lysates were collected and then added equal volumes to incubate with GST–Rhotekin–RBD and glutathione–sepharose beads according to the manufacturer's instructions. Activated GTP–RhoA proteins bound to beads in cell lysates were precipitated and then subjected to Western blot using specific anti-RhoA antibody. The levels of active RhoA were determined by normalizing with the total RhoA proteins present in the cell lysates.

2.11. Transfection

Control siRNA (5′-UUCUCCGAACGUGUCACGU-3′) and RhoA siRNA (5′-CGGAAUGAUGAGCACACAA-3′) were purchased from Qiagen Inc. (Valencia, CA) that were used for transfection by using Lipofectamine™ 2000 (Invitrogen) according to the manufacturer's recommendations.

Table 1
The actions of various cytoskeleton blockers.

Compounds	Effects			
	Microtubule polymerization	Microtubule depolymerization	Actin polymerization	Actin depolymerization
Paclitaxel	+[a]	–	–	–
Colchicine	–	+[b]	–	–
Cytochalasin B[c]	–	–	–	+[d]
Phallacidin	–	–	+[e]	–
PT–262	–	–	+[f]	–

[a] Induction of mitotic arrest by inhibiting spindle function but not inducing cell elongation.
[b] Induction of mitotic arrest by inhibiting spindle function but not inducing cell elongation.
[c] A cytokinesis inhibitor induces actin depolymerization.
[d] Cytochalasin B inhibits actin polymerization and cytokinesis.
[e] Cell elongation by inducing direct binding to F-actin.
[f] Cell elongation by inducing abnormal actin polymerization but did not directly bind to F-actin.

2.12. Statistical analysis

All results were obtained from at least three separate experiments. Data were analyzed by one-way or two-way analysis of variance (ANOVA), and further post hoc tests using the statistic software of GraphPad Prism 4 (GraphPad software, Inc. San Diego, CA). A p value of <0.05 was considered as statistically significant in each experiment.

3. Results

3.1. PT-262 induces the cytoskeleton alteration and cell elongation in lung carcinoma cells

As shown in Fig. 1A, treatment with 2 μM PT-262 dramatically induced cytoskeleton alteration in A549 lung cancer cells. The cells were elongated and formed an abnormal cytoskeleton following

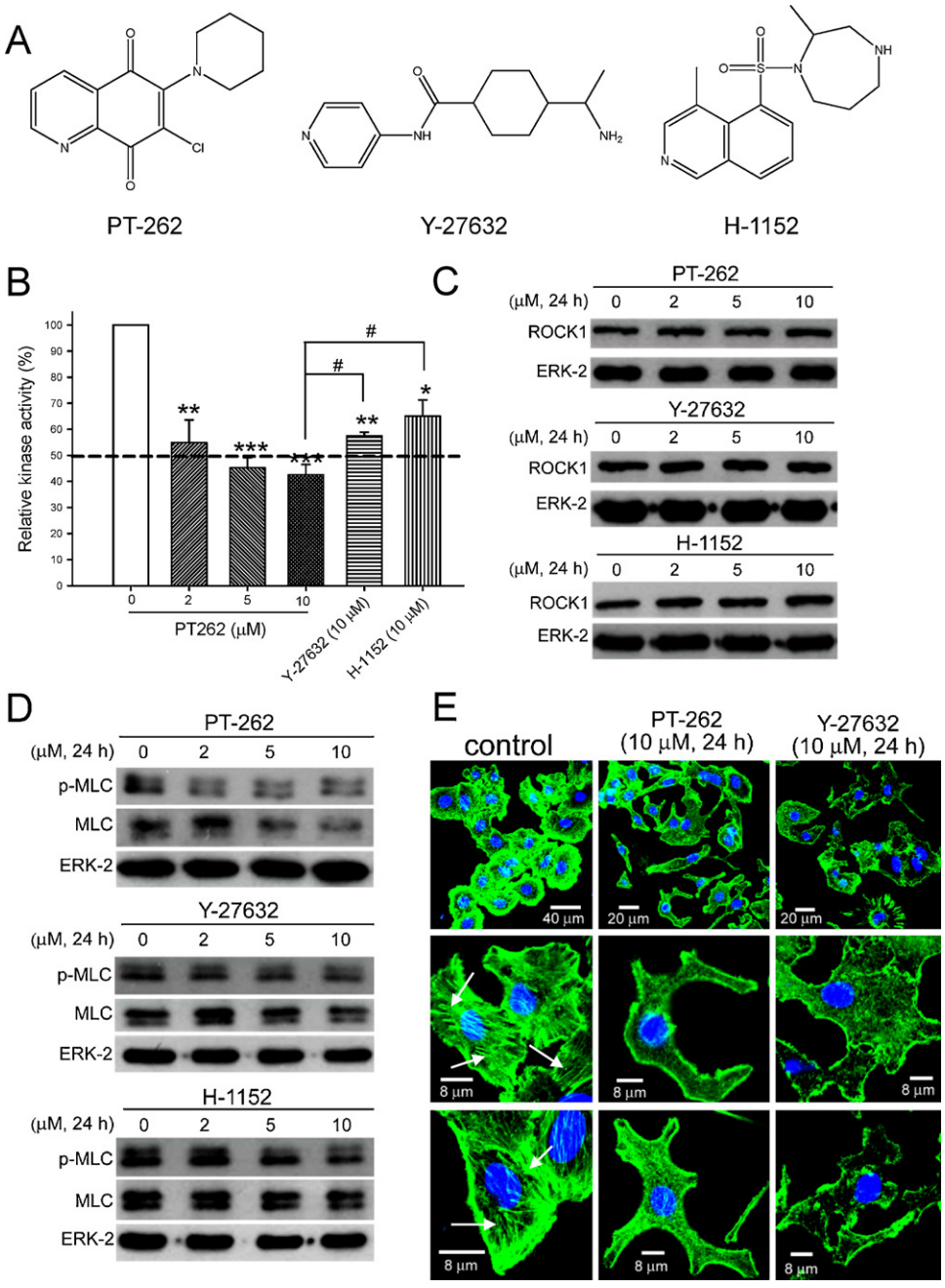

Fig. 3. Effect of PT-262 on the ROCK kinase activity, phospho-MLC and total-MLC expression, and stress fibers in lung carcinoma cells. (A) Chemical structures of PT-262, Y-27632, and H-1152. (B) A549 cells were treated with or without PT-262, Y-27632 and H-1152. At the end of the treatments, the cell lysates were subjected to ROCK kinase activity assays. The amount of phosphorylated MBS was calculated in a binding reaction with a horseradish peroxidase conjugated an anti-phospho-MBS threonine-696 specific antibody, which catalyzes the chromogenic substrate tetra-methylbenzidine to blue-color. Results were obtained from 3 separate experiments. The bar represents the mean ± S.E. $^{*}p < 0.05$, $^{**}p < 0.01$, and $^{***}p < 0.001$ indicate significant difference between control and inhibitor treated samples. $^{\#}p < 0.05$ indicates a significant difference between PT-262 and ROCK inhibitor (Y-27632 or H-1152) treated samples. (C) and (D), A549 cells were treated with or without 2–10 μM PT-262, Y-27632, and H-1152. Representative Western blot data of the protein levels of ROCK1, phospho-MLC, and total MLC were shown from one of three separate experiments with similar findings. (E) F-actin proteins were stained with BODIPY FL phallacidin, which displayed a green color. The nuclei were stained with Hoechst 33258, which displayed a blue color. The arrows indicate the location of stress fibers. (For interpretation of the references to color in this sentence, the reader is referred to the web version of the article.)

exposure to PT-262. To view the elaborate structure of cell morphology, the cells were observed by confocal microscope combined Bio-AFM. The cytoskeleton alteration and cell elongation were clearly induced by PT-262 by comparison with the untreated sample (Fig. 1B). The green color exhibited by F-actin formed an elongated shape after treatment with 2 μM PT-262 for 24 h. The magnified pictures of the circle marks in Fig. 1B show the fork shape in the elongated cell (Fig. 1C). Cell length elongated to ~160 μm following treatment with 2 μM PT-262 (Fig. 1D). Moreover, PT-262 increased the formation of F-actin concentrated spikes (Fig. 1D, arrows). The average cell length was extended from 39.15 to 65.30 μm following treatment with PT-262 by calculating the long diameter (Fig. 1E).

3.2. Various cytoskeleton inhibitors induce cytoskeleton remodeling and morphological alteration

To investigate the cytoskeleton alteration by PT-262, A549 cells were compared with various cytoskeleton blockers, including paclitaxel, colchicine, and phallacidin. β-tubulin and F-actin were displayed by staining with Cy3-labeled mouse anti-β-tubulin and BODIPY FL phallacidin, respectively. Treatment with 50 nM paclitaxel for 24 h increased the red fluorescence intensity of β-tubulin by inducing the microtubule polymerization (Fig. 2). In contrast, colchicine (50 nM, 24 h) reduced the red intensity of β-tubulin by the inhibition of microtubulin polymerization (Fig. 2). Phallacidin (0.5 U/ml, 24 h) increased the green fluorescence

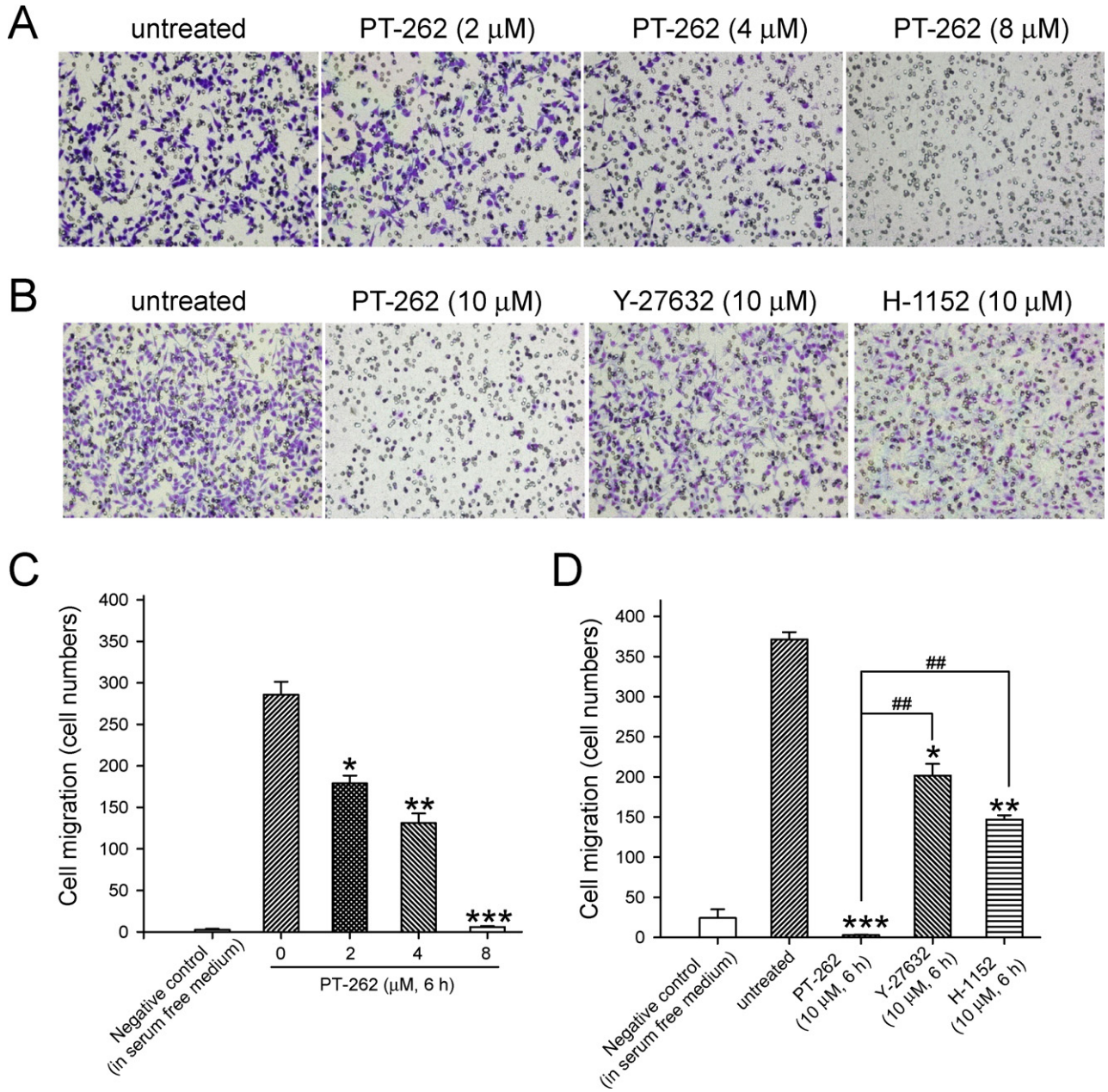

Fig. 4. Effect of PT-262 on cell migration by Boyden chamber analysis in lung carcinoma cells. (A) A549 cells were treated with or without 2–8 μM PT-262 for 6 h. (B) A549 cells were treated with or without 10 μM PT-262, Y-27632 or H-1152 for 6 h. At the end of treatment, the migrated cells on the lower surface of membranes were stained with hematoxylin and observed under a light microscope. Gray color spots indicate 8 μm pores on the polycarbonate membranes. The migrated cells indicate purple color. (C) and (D), the migrated cells on the lower surface were counted after stained with hematoxylin under a light microscope. Results were obtained from 3 separate experiments. The bar represents the mean ± S.E. $^{*}p < 0.05$, $^{**}p < 0.01$, and $^{***}p < 0.001$ indicate a significant difference between control and inhibitor treated samples. $^{\#\#}p < 0.05$ indicates a significant difference between PT-262 and ROCK inhibitor (Y-27632 or H-1152) treated samples. (For interpretation of the references to color in this sentence, the reader is referred to the web version of the article.)

intensity of F-actin by promoting actin polymerization and caused cell elongation in A549 cells. PT-262 was similar to phallacidin on the cell elongation (Fig. 2). Phallacidin (0.5 U/ml) increased 88.4% of actin polymerization than control using actin polymerization assays *in vitro*; nonetheless, treatment with 2–10 μM PT-262 did not alter actin polymerization. Cytochalasin B inhibited actin polymerization and cytokinesis but without inducing cell elongation in A549 cells [25]. The actions of these cytoskeleton inhibitors are summarized in Table 1.

3.3. PT-262 inhibits ROCK kinase activity and stress fiber formation

The chemical structures of PT-262, Y-27632, and H-1152 are shown in Fig. 3A. Treatment with 2–10 μM PT-262 inhibited ROCK kinase activities via a concentration-dependent manner in A549 cells (Fig. 3B). Furthermore, PT-262 was more effective on inhibiting ROCK kinase activities than Y-27632 and H-1152 (Fig. 3B, $p < 0.05$). The IC_{50} value (the concentration of 50% kinase activity inhibition) was around 5 μM by PT-262; the IC_{50} values of Y-27632 and H-1152 were >10 μM. Nonetheless, PT-262, Y-27632, and H-1152 did not reduce ROCK protein expression (Fig. 3C). ERK-2 protein has been used as an internal control [24,26]. The protein level of ERK-2 was not altered by PT-262 (Fig. 3C). In addition, treatment with 5–10 μM PT-262 decreased the levels of phospho-MLC and total MLC proteins (Fig. 3D). Y-27632 and H-1152 also decreased the MLC protein expression. The formation of stress fibers was found in the PT-262-untreated cells (Fig. 3E, arrows); in contrast, PT-262 or Y-27632 can block the stress fiber formation completely (Fig. 3E).

3.4. PT-262 inhibits cancer cell migration

To examine the effect of PT-262 on cancer cell migration, the cells were examined by Boyden chamber analysis. Treatment with 2–10 μM PT-262 for 6 h significantly blocked the cell migration in a concentration-dependent manner (Fig. 4A and C). The negative control of cell migration was used by incubating in serum free medium. Moreover, PT-262 was more effective in inhibiting cell migration than Y-27632 and H-1152 (Fig. 4B and Fig. 4D). The migration inhibition of PT-262 was verified by the wound-healing assay. As shown in Fig. 5A Fig. 5, the wound width by the cell migration was observed under a phase contrast microscope following treatment with 2 μM PT-262 for 8 h or 24 h. PT-262 significantly increased the wound width than untreated samples (Fig. 5B).

3.5. Blockage of RhoA expression inhibits cancer cell migration

Transfection with 20–80 nM RhoA siRNA for 48 h decreased RhoA gene expression and protein levels in A549 cells (Fig. 6A and C). The blockage of RhoA expression inhibited cell migration via a concentration-dependent manner (Fig. 6B). Furthermore, the phospho-MLC and total MLC proteins also were reduced by transfection with RhoA siRNA (Fig. 6B). The ROCK protein expression was not altered by RhoA siRNA (Fig. 6C). The effect of PT-262 on RhoA GTPase activity was further analyzed by RhoA pull-down assays. However, treatment with PT-262, Y-27632 and H-1152 did not significantly alter the RhoA GTPase activity and protein expression (Fig. 6D and E).

4. Discussion

The RhoA–ROCK pathway has been shown to promote cancer cell migration, invasion and metastasis. The RhoA–ROCK pathway is a potential target for cancer chemotherapy. In this study, we provide a newly synthesized compound, PT-262, that markedly induces cytoskeleton remodeling, cell elongation, and migration inhibition in human lung carcinoma cells. The concentration range of PT-262 at 2–10 μM blocked ROCK kinase activity and cancer cell migration in a concentration-dependent manner. Interestingly, PT-262 is more effective in inhibiting the ROCK kinase activity and migration than ROCK inhibitors Y-27632 and H-1152. The findings provide that PT-262 is a novel and potent ROCK inhibitor.

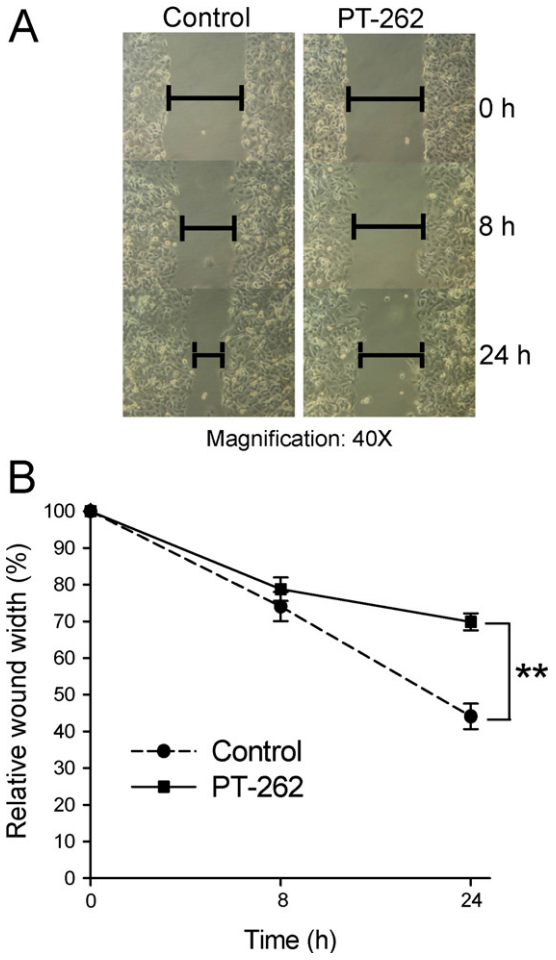

Fig. 5. Effect of PT-262 on cell migration by wound healing assay in lung carcinoma cells. (A) The confluent cell monolayer scraped by a pipette tip to generate wounds of 6–7 mm. Then the cells were treated with or without 8 μM PT-262 and then re-cultured for various periods. Photographs were taken at the same position of the wound. (B) Results were obtained from 3 separate experiments. The bar represents the mean ± S.E. $^{**}p < 0.01$ indicates a significant difference between the control and PT-262 treated samples.

Small RhoGTPases are key regulators of cytoskeleton dynamics [1,2]. RhoA is a key family of RhoGTPases that is involved in the regulation of cytoskeleton reorganization [5,6]. Overexpression of RhoA has been shown in various cancers [7]. ROCK is a downstream effector protein of RhoA [5]. The Rho–ROCK signaling pathway participates in cancer cell migration and transformation [27]. Blockage of RhoA expression can prevent cell migration in A549 lung cancer cells. However, PT-262 inhibited ROCK kinase activity but did not alter RhoA GTPase activity and protein expression. ROCK can regulate the activity of MLC proteins by direct MLC phosphorylation [9,10]. Cell migration of actomyosin contractility is mediated by the phosphorylation of MLC [1]. The inhibition of ROCK function by PT-262 reduced the protein levels of MLC and phosphorylated MLC. Also, PT-262 prevented stress fiber formation in lung cancer cells. Thus, these results show that PT-262 can prevent cancer cell migration by blocking the ROCK-MLC signaling pathway.

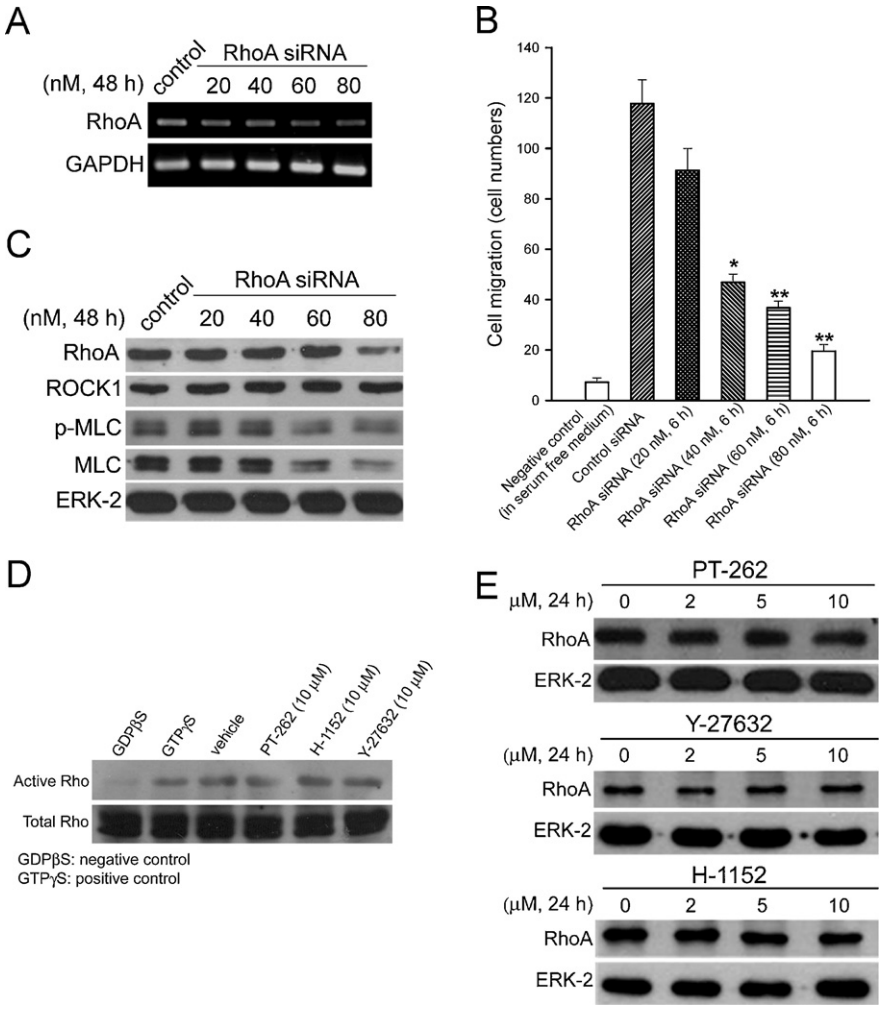

Fig. 6. Effect of PT-262 on RhoA GTPase activity and protein expression in lung carcinoma cells. (A) A549 cells were transfected with 20–80 nM control or RhoA siRNA for 48 h. The RhoA gene expression was analyzed by RT-PCR. GAPDH was an internal control gene. (B) The cell migration was examined by Boyden chamber analysis following transfection with control or RhoA siRNA. Results were obtained from 3 separate experiments. The bar represents the mean ± S.E. $^{*}p < 0.05$ and $^{**}p < 0.01$ indicate a significant difference between the control and RhoA siRNA treated samples. (C) The protein levels of RhoA, ROCK1, phospho-MCL, MLC, and ERK-2 were analyzed by Western blot. (D) RhoA GTPase activity was detected by a RhoA-GTP pull-down assay kit according to the manufacturer's instructions. A549 cells were treated with or without 10 μM PT-262, Y-27632 and H-1152. Activated RhoA-GTP and total RhoA in cell lysates were detected by Western blot using anti-RhoA. GDPβS and GTPγS were used as a negative control and positive control, respectively. (E) A549 cells were treated with or without 2–10 μM PT-262, Y-27632 and H-1152. At the end of treatment, the protein levels of RhoA and ERK-2 were analyzed by Western blot. The data are shown from one of three separate experiments with similar findings.

The cytoskeleton proteins of microtubules and F-actin are potential targets for cancer chemotherapy [2,28]. The disruption of F-actin has been found in malignant transformed cells [2]. Actin polymerization and remodeling play a critical role in the morphologic and phenotypic events in cancer cells [2,28]. Chemotherapeutic drugs that target cytoskeleton remodeling can prevent malignant transformation and metastasis processes. Paclitaxel is an effective anticancer drug that acts by stabilizing microtubules and inducing formation of microtubule bundles to block mitosis [29,30]. The vinca alkaloids and colchicine induce mitotic arrest by inhibiting microtubule polymerization and disassembling mitotic spindle [28,31]. Cytochalasins bind to the plus end of F-actin, reduce F-actin mass, and prevent actin polymerization [28,32]. Malignant cells are reported to be more sensitive to cytochalasin B than normal cells [28,33]. Phalloidins can bind to F-actin to inhibit actin depolymerization [32]. Among these cytoskeleton blockers, we found paclitaxel and colchicine induced microtubule polymerization and depolymerization, respectively. However, phallacidin promoted actin polymerization by stabilizing F-actin to induce the cell elongation in lung cancer cells. Interestingly, PT-262 increased cell elongation in a manner comparable to phallacidin treatment, indicating that PT-262 may act in a similar fashion, promoting F-actin stability. Nonetheless, PT-262 did not bind to F-actin directly using actin polymerization *in vitro* assays. Therefore, we suggest that PT-262 blocks cytoskeleton functions indirectly by inhibiting ROCK signaling.

The ROCK1 protein crystal structure has been reported [10]. It has been shown that four crystal structures contain ATP-competitive inhibitors of ROCK1 in the third pocket site [10]. Fig. 7A shows a computational structure model of the interaction of PT-262 and ROCK1 protein. The 3D structures of ROCK inhibitors on the binding site of ROCK1 were utilized for docking analysis [10]. The coordinates of binding-pocket atoms were taken from the PDB for the docking tools such as GEMDOCK [34,35]. Furthermore, the potential binding sites were predicted by using Q-SiteFinder, which was an energy-based method for the prediction of protein–ligand binding sites [36,37]. We have further compared the binding of PT-262, H-1152, and Y-27632 to ROCK1 (Supplementary Fig. 1). The nitrogen atoms on the quinoline group of PT-262, the pyridine group of H-1152, and the isoquinoline group of Y-27632 all form hydrogen bonds with the nitrogen on the main chain of M156. Three functional groups occupy the same space as the adenine of ATP occupies (Supplementary Fig. 1). In addition, the chlorine and quinoline moieties of PT-262 contact with the MET153 amino

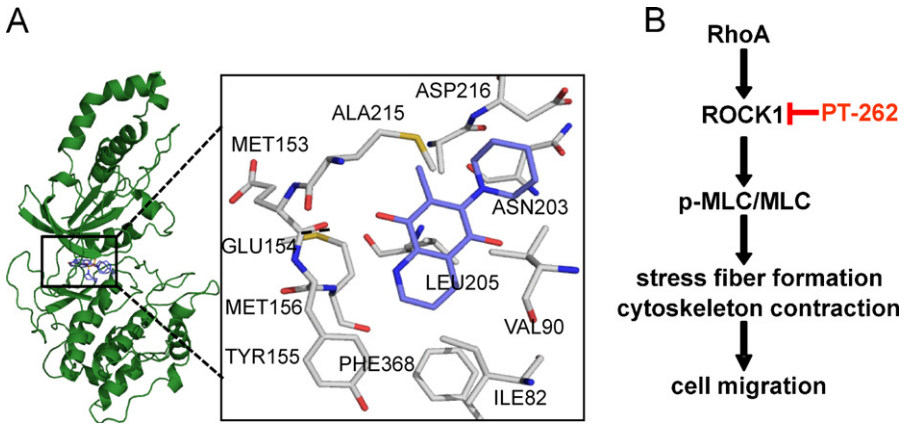

Fig. 7. A proposed model of PT-262 on the inhibition of ROCK. (A) A computational model of the interaction of PT-262 (blue color) and ROCK protein (green color). (B) The inhibition of ROCK signaling pathway by PT-262. (For interpretation of the references to color in this sentence, the reader is referred to the web version of the article.)

residue, and the chlorine and piperidin moieties of PT-262 contact with ALA215 amino residue, which may determine the selectivity at the ROCK inhibition. The chlorine of PT-262 may be the reason more effective on inhibition of ROCK activity than Y-27632 and H-1152. Accordingly, the computational model supports the findings that PT-262 blocks the ROCK kinase activities by binding on ATP-binding site.

The derivatives of quinolinediones have been shown to possess many biological activities including anti-tumor actions. For example, 6-anilino-5,8-quinolinedione (LY83583) is an inhibitor of guanylyl cyclase that can prevent cancer cell proliferation [20]. In addition, 6-chloro-7-(2-morpholin-4-ylethylamino) quinoline-5,8-dione (NSC 663284) is an inhibitor of CDC25 protein phosphatases that mediates cell cycle arrest by reducing CDC2 activation [21]. In this report, we provide a novel function of quinolinedione derivatives that is a ROCK inhibitor.

In conclusion, we presented a model of the inhibition of ROCK and its downstream regulation of cell migration by PT-262 (Fig. 7B). The model provides a novel mechanism of cell migration inhibition by the 5,8-quinolinedione derivative through the irreversible effects of cytoskeleton alteration and cell elongation in blocking ROCK pathway.

Acknowledgment

This work was supported by the grant from NSC 96-2311-B-320-006-MY3, Taiwan.

Appendix A. Supplementary data

Supplementary data associated with this article can be found, in the online version, at doi:10.1016/j.bcp.2011.01.009.

References

[1] Hall A. Rho GTPases and the actin cytoskeleton. Science 1998;279:509–14.
[2] Rao J, Li N. Microfilament actin remodeling as a potential target for cancer drug development. Curr Cancer Drug Targets 2004;4:345–54.
[3] Hall A. Signal transduction through small GTPases—a tale of two GAPs. Cell 1992;69:389–91.
[4] Ridley AJ, Hall A. The small GTP-binding protein rho regulates the assembly of focal adhesions and actin stress fibers in response to growth factors. Cell 1992;70:389–99.
[5] Wyckoff JB, Pinner SE, Gschmeissner S, Condeelis JS, Sahai E. ROCK- and myosin-dependent matrix deformation enables protease-independent tumor-cell invasion *in vivo*. Curr Biol 2006;16:1515–23.
[6] Narumiya S, Tanji M, Ishizaki T. Rho signaling, ROCK and mDia1, in transformation, metastasis and invasion. Cancer Metastasis Rev 2009;28:65–76.
[7] Sahai E, Marshall CJ. RHO-GTPases and cancer. Nat Rev Cancer 2002;2:133–42.
[8] Leung T, Chen XQ, Manser E, Lim L. The p160 RhoA-binding kinase ROK alpha is a member of a kinase family and is involved in the reorganization of the cytoskeleton. Mol Cell Biol 1996;16:5313–27.
[9] Kawano Y, Fukata Y, Oshiro N, Amano M, Nakamura T, Ito M, et al. Phosphorylation of myosin-binding subunit (MBS) of myosin phosphatase by Rho-kinase *in vivo*. J Cell Biol 1999;147:1023–38.
[10] Jacobs M, Hayakawa K, Swenson L, Bellon S, Fleming M, Taslimi P, et al. The structure of dimeric ROCK I reveals the mechanism for ligand selectivity. J Biol Chem 2006;281:260–8.
[11] Amano M, Chihara K, Kimura K, Fukata Y, Nakamura N, Matsuura Y, et al. Formation of actin stress fibers and focal adhesions enhanced by Rho-kinase. Science 1997;275:1308–11.
[12] Liu S, Goldstein RH, Scepansky EM, Rosenblatt M. Inhibition of rho-associated kinase signaling prevents breast cancer metastasis to human bone. Cancer Res 2009;69:8742–51.
[13] Uehata M, Ishizaki T, Satoh H, Ono T, Kawahara T, Morishita T, et al. Calcium sensitization of smooth muscle mediated by a Rho-associated protein kinase in hypertension. Nature 1997;389:990–4.
[14] Ishizaki T, Uehata M, Tamechika I, Keel J, Nonomura K, Maekawa M, et al. Pharmacological properties of Y-27632, a specific inhibitor of rho-associated kinases. Mol Pharmacol 2000;57:976–83.
[15] Takamura M, Sakamoto M, Genda T, Ichida T, Asakura H, Hirohashi S. Inhibition of intrahepatic metastasis of human hepatocellular carcinoma by Rho-associated protein kinase inhibitor Y-27632. Hepatology 2001;33:577–81.
[16] Somlyo AV, Bradshaw D, Ramos S, Murphy C, Myers CE, Somlyo AP. Rho-kinase inhibitor retards migration and *in vivo* dissemination of human prostate cancer cells. Biochem Biophys Res Commun 2000;269:652–9.
[17] Chang HR, Huang HP, Kao YL, Chen SL, Wu SW, Hung TW, et al. The suppressive effect of Rho kinase inhibitor Y-27632, on oncogenic Ras/RhoA induced invasion/migration of human bladder cancer TSGH cells. Chem Biol Interact 2010;183:172–80.
[18] Sasaki Y, Suzuki M, Hidaka H. The novel and specific Rho-kinase inhibitor (S)-(+)-2-methyl-1-[(4-methyl-5-isoquinoline)sulfonyl]-homopiperazine as a probing molecule for Rho-kinase-involved pathway. Pharmacol Ther 2002;93:225–32.
[19] Yoon E, Choi HY, Shin KJ, Yoo KH, Chi DI, Kim DJ. The regioselectivity in the reaction of 6,7-dihaloquinoline-5,8-diones with amine nucleophiles in various solvents. Tetrahedron Lett 2000;41:7475–80.
[20] Lodygin D, Menssen A, Hermeking H. Induction of the Cdk inhibitor p21 by LY83583 inhibits tumor cell proliferation in a p53-independent manner. J Clin Invest 2002;110:1717–27.
[21] Lazo JS, Aslan DC, Southwick EC, Cooley KA, Ducruet AP, Joo B, et al. Discovery and biological evaluation of a new family of potent inhibitors of the dual specificity protein phosphatase Cdc25. J Med Chem 2001;44:4042–9.
[22] Fang Y, Linardic CM, Richardson DA, Cai W, Behforouz M, Abraham RT. Characterization of the cytotoxic activities of novel analogues of the antitumor agent, lavendamycin. Mol Cancer Ther 2003;2:517–26.
[23] Hsu TS, Chen C, Lee PT, Chiu SJ, Liu HF, Tsai CC, et al. 7-Chloro-6-piperidin-1-yl-quinoline-5,8-dione (PT-262), a novel synthetic compound induces lung carcinoma cell death associated with inhibiting ERK and CDC2 phosphorylation via a p53-independent pathway. Cancer Chemother Pharmacol 2008;62:799–808.
[24] Chao JI, Kuo PC, Hsu TS. Down-regulation of survivin in nitric oxide-induced cell growth inhibition and apoptosis of the human lung carcinoma cells. J Biol Chem 2004;279:20267–76.
[25] Chao JI, Liu HF. The blockage of survivin and securin expression increases the cytochalasin B-induced cell death and growth inhibition in human cancer cells. Mol Pharmacol 2006;69:154–64.
[26] Kuo PC, Liu HF, Chao JI. Survivin and p53 modulate quercetin-induced cell growth inhibition and apoptosis in human lung carcinoma cells. J Biol Chem 2004;279:55875–8.
[27] Li B, Zhao WD, Tan ZM, Fang WG, Zhu L, Chen YH. Involvement of Rho/ROCK signalling in small cell lung cancer migration through human brain microvascular endothelial cells. FEBS Lett 2006;580:4252–60.

[28] Jordan MA, Wilson L. Microtubules and actin filaments: dynamic targets for cancer chemotherapy. Curr Opin Cell Biol 1998;10:123–30.
[29] Schiff PB, Horwitz SB. Taxol stabilizes microtubules in mouse fibroblast cells. Proc Natl Acad Sci USA 1980;77:1561–5.
[30] Jordan MA, Toso RJ, Thrower D, Wilson L. Mechanism of mitotic block and inhibition of cell proliferation by taxol at low concentrations. Proc Natl Acad Sci USA 1993;90:9552–6.
[31] Dhamodharan R, Jordan MA, Thrower D, Wilson L, Wadsworth P. Vinblastine suppresses dynamics of individual microtubules in living interphase cells. Mol Biol Cell 1995;6:1215–29.
[32] Cooper JA. Effects of cytochalasin and phalloidin on actin. J Cell Biol 1987;105:1473–8.
[33] Stournaras C, Stiakaki E, Koukouritaki SB, Theodoropoulos PA, Kalmanti M, Fostinis Y, et al. Altered actin polymerization dynamics in various malignant cell types: evidence for differential sensitivity to cytochalasin B. Biochem Pharmacol 1996;52:1339–46.
[34] Yang JM, Chen CC. GEMDOCK: a generic evolutionary method for molecular docking. Proteins 2004;55:288–304.
[35] Yang JM. Development and evaluation of a generic evolutionary method for protein–ligand docking. J Comput Chem 2004;25:843–57.
[36] Laurie AT, Jackson RM. Q-SiteFinder: an energy-based method for the prediction of protein–ligand binding sites. Bioinformatics 2005;21:1908–16.
[37] Huang B, Schroeder M. LIGSITEcsc: predicting ligand binding sites using the Connolly surface and degree of conservation. BMC Struct Biol 2006;6:19.